Provided for non-commercial research and education use.
Not for reproduction, distribution or commercial use.

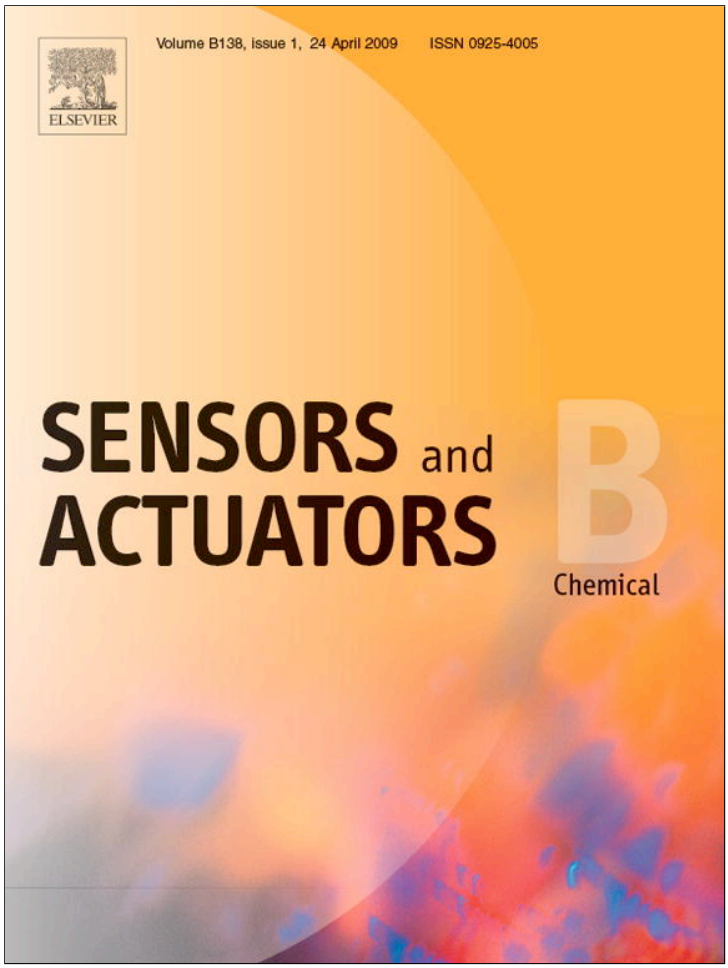

This article appeared in a journal published by Elsevier. The attached copy is furnished to the author for internal non-commercial research and education use, including for instruction at the authors institution and sharing with colleagues.

Other uses, including reproduction and distribution, or selling or licensing copies, or posting to personal, institutional or third party websites are prohibited.

In most cases authors are permitted to post their version of the article (e.g. in Word or Tex form) to their personal website or institutional repository. Authors requiring further information regarding Elsevier's archiving and manuscript policies are encouraged to visit:

http://www.elsevier.com/copyright

Author's personal copy

Sensors and Actuators B 138 (2009) 64–70

Contents lists available at ScienceDirect

Sensors and Actuators B: Chemical

journal homepage: www.elsevier.com/locate/snb

An optical MEMS sensor utilizing a chitosan film for catechol detection

Peter Dykstra[a], Junjie Hao[b], Stephan T. Koev[a], Gregory F. Payne[c], Liangli Yu[d], Reza Ghodssi[a,*]

[a] Department of Electrical and Computer Engineering, Institute for Systems Research, University of Maryland, College Park, MD 20742, USA
[b] Department of Chemistry and Biochemistry, University of Maryland, College Park, MD 20742, USA
[c] University of Maryland Biotechnology Institute, College Park, MD 20742, USA
[d] Department of Nutrition and Food Science, University of Maryland, College Park, MD 20742, USA

ARTICLE INFO

Article history:
Received 31 July 2008
Received in revised form 23 January 2009
Accepted 30 January 2009
Available online 13 February 2009

Keywords:
Chitosan
Catechol
SU-8 waveguides
Absorbance measurements
Optical fibers

ABSTRACT

Catechol is a widely studied phenol that is a common byproduct of factory waste. The presence of catechol in drinking water and food poses a safety concern due to its toxic and possibly carcinogenic effects. We report the successful fabrication and testing of an optical MEMS sensor for the detection of catechol. Studies on catechol detection have shown that byproducts from catechol oxidation will react with a chitosan film and induce a significant absorbance change in the UV and near UV range. Our reported sensor takes advantage of this unique absorbance property to detect catechol by measuring the change in light intensity at 472 nm through an electrodeposited film of chitosan on a transparent, conductive film of indium tin oxide. This optical detection technique eliminates the nonspecific response from the common antioxidant, ascorbic acid, which does not cause an absorbance change. Absorbance measurements were performed over 10 min while applying an oxidizing current density of 4 A/m^2. We observed a considerable response even for our lowest measured concentration (1 mM) while the detection limit of the device is found to be about 0.2 mM for a 10 min reaction time.

© 2009 Elsevier B.V. All rights reserved.

1. Introduction

Monitoring the safety of our water supply by using portable, efficient and inexpensive devices has become an area of growing interest over the past decade. The growth of industry has contributed to the contamination of ground waters with various potentially dangerous organic chemicals [1]. Catechol is a phenolic compound commonly generated in factory processes which has been proven to have detrimental health effects [2–4]. Efforts to monitor the existence of such compounds are typically expensive and time-consuming since most analysis must be performed in an off-site laboratory requiring high equipment and labor costs. One solution to this problem is through the use of microelectromechanical systems (MEMS) to create on-chip sensors which can give field personnel accurate and sensitive data on-site regarding the testing of the water supply.

Recently reported sensors for catechol detection either use optical or electrochemical measurement schemes. Optical sensors making use of both absorbance [5] and fluorescence [6] detection have been reported, but the necessity for bulky, external measuring equipment has hindered the fabrication of such devices on chip. Electrophoresis for catechol detection has also been performed on patterned electrodes in a microfluidic channel [7]. Electrochemical sensors typically employ a standard three electrode system with the working electrode covered by an immobilization matrix such as calcium carbonate [8], polypyrrole [9], and organoclay [10]. Ion-exchanging membranes such as Nafion have also been reported [11]. These materials entrap an oxidizing enzyme (most commonly polyphenol oxidase [12,13]) in order to chemically oxidize the catechol allowing the reduction reaction at the electrode to be measured. Although these devices can result in high sensitivity and selectivity, the enzyme activity degrades over time and can be directly affected by certain conditions such as the pH of the solution [1,10].

Our reported device utilizes an optical absorbance technique in a sealed microfluidic channel for the detection of catechol. In order to amplify the effect of the detected absorbance by catechol oxidation, the aminopolysaccharide chitosan is deposited onto a transparent, conductive film of indium tin oxide (ITO) in the microfluidic channel thus intersecting the pathway of the light through the device. A 4 A/m^2 current density is used to control both the electrodeposition of the chitosan film and the oxidation of the catechol molecules at the ITO-chitosan interface as shown schematically in Fig. 1. The products of oxidized catechol (*o*-quinones) covalently bond to chitosan's amine groups to create a measurable absorbance change. The proposed detection scheme does not require the use of any enzymes yet still remains selective to phenolic compounds vs. common reducing agents such as ascorbic acid. There is no evidence to support that the deposited chitosan films degrade over time and

* Corresponding author. Tel.: +1 301 405 8158; fax: +1 301 314 9218.
E-mail addresses: pdykstra@umd.edu (P. Dykstra), ghodssi@umd.edu (R. Ghodssi).

0925-4005/$ – see front matter © 2009 Elsevier B.V. All rights reserved.
doi:10.1016/j.snb.2009.01.065

Author's personal copy

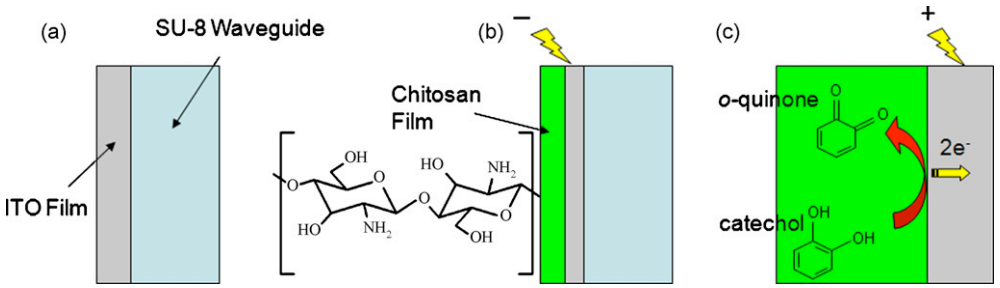

Fig. 1. (a) Scheme demonstrating the ITO film on the facet of an SU-8 waveguide. (b) By applying a negative current bias, a solid, transparent film of chitosan (with shown chemical structure) is electrodeposited onto the ITO electrode. (c) A blown up view of the chitosan–ITO interface demonstrates catechol diffusion through the chitosan matrix and electrochemical oxidation by a positive current bias applied to the ITO electrode.

multiple sites can be patterned in the same channel allowing for many uses from one chip [14].

We first quantified the measured absorbance due to catechol oxidation using bench top instruments and compared these results to the data collected with the MEMS sensor. We also demonstrated the necessity for the chitosan film through absorbance experiments without the film. Finally, we investigate the selectivity of the device response for an easily oxidized chemical, ascorbic acid.

2. Materials and theory

2.1. Catechol

Catechol is a benzenediol, which is a subset of the phenol class of organic compounds. The chemical structure of benzenediols contains a benzene ring with two attached hydroxyl (OH–) groups. Specifically, the chemical formula of catechol is $C_6H_6O_2$. During oxidation, catechol loses its hydrogen atoms from the hydroxyl groups and becomes an orthobenzoquinone, more commonly referred to as an *o*-quinone. Phenols comprise numerous different compounds most of which exhibit antioxidant qualities. While the antioxidant properties of some phenols contribute to healthy cell respiration [15–17], catechol can cause damage for several reasons. First, catechol has a non-polar structure which allows the molecules to be easily taken up by the cells, but not easily expelled. This leads to an accumulation of catechol in the cell. Secondly, the *o*-benzoquinones generated upon catechol oxidation may react with vital cellular components such as lipids, proteins and DNA and cause damage to cells [18].

2.2. Chitosan

Chitosan is a unique material that is well suited for biological micro-devices due to its ability to be selectivity deposited and its high density of amine groups, which provide active bonding sites [14,19]. The selective deposition is attributed to chitosan's insolubility above a pH of 6.5. At low pH, chitosan is protonated and soluble in water. As the pH rises above 6.5, the amino groups lose their net positive charge and the chitosan becomes insoluble. By taking advantage of this property, one can deposit a film of chitosan onto a cathode during an electrochemical reaction. The pH rises with increasing proximity to the cathode due to the reduction of the hydrogen ions. The chitosan forms as a thin film or hydrogel over the cathode surface depending on the amplitude of the applied current density and remains stable even after the current has been removed.

Although other patterning techniques have been explored for chitosan including nanoimprint lithography [20], and reactive ion etching [21], electrodeposition has the advantage of not subjecting the chitosan to any processing which can damage or contaminate the surface amine groups, and it can be performed on non-planar surfaces as demonstrated in this work. In addition, the possible C2 nucleophilic amino groups ($-NH_2$) of the glucosamine unit, the repeating monosugar residue of chitosan, react with the carbonyl groups of the *o*-quinones formed from the oxidized catechol molecules. This reaction alters the physicochemical properties of the chitosan molecule and imparts physical changes to the film, such as a change in the optical absorbance [22,23].

2.3. Optics

Understanding the operating principle of the device requires a more detailed understanding of light propagation and absorption through a medium. Absorbance can be related to the concentration of absorbing species present as demonstrated by the Beer–Lambert law:

$$A = -\log_{10}\left(\frac{I_1}{I_0}\right) = \varepsilon l c \quad (1)$$

where ε is the molar absorptivity, l is the path length the light takes as it propagates through the absorbing layer and c is the concentration. In our experiments, the path length, l, is defined as the thickness of the deposited chitosan film. This assumption is made since the absorbing analytes are only contained within the chitosan film while there is no absorbance change over time occurring anywhere else on the path that the light takes through the device. *o*-Quinones have been reported to show a strong absorbance in the UV and near UV range of the electromagnetic spectrum [22]. For this reason, a blue laser source at 472 nm was chosen for the optical measurements taken with the MEMS sensor.

In our device, on-chip waveguides are patterned from the polymer SU-8 as shown in the device schematic (Fig. 2). Blue light is coupled in and out of the waveguides via multimode fibers with a core diameter of 62.5 μm. The cross-sectional area of the polymer waveguides are 100 μm × 150 μm. The light propagates through a film of chitosan that has been deposited onto a transparent, conductive film of indium tin oxide. The cross-sectional area of the polymer waveguides is large compared to the wavelength of light (visible), therefore we can

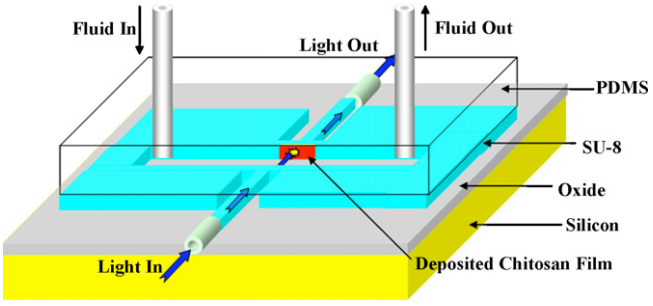

Fig. 2. Layer-by-layer schematic of the packaged device.

Author's personal copy

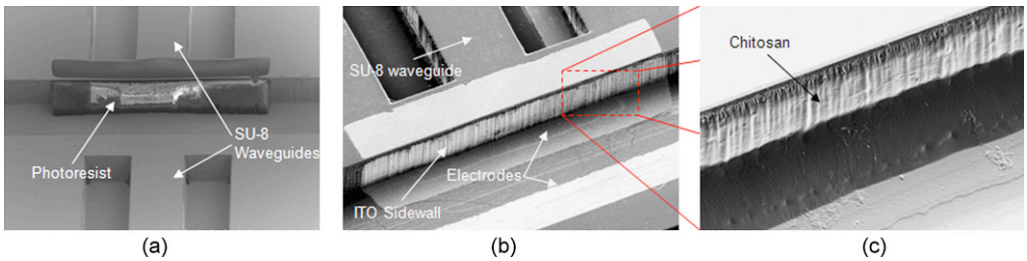

Fig. 3. (a) Photoresist patterned along the sidewall of the microfluidic channel demonstrating good coverage along the height of the wall. (b) Following the etching of the exposed ITO, only a portion covering the waveguide facet remains. (c) Chitosan deposition at 4 A/m^2 for 10 min covers the sidewall.

use geometrical optics assumptions to model the light propagation.

Since the absorbance measurement is dependent on the optical power being received, it is important to understand the different optical loss mechanisms through the device in order to achieve an acceptable signal to noise ratio. The primary sources of loss are caused by waveguiding losses which include material absorption and scattering, divergence of the light crossing the channel, and roughness associated with the waveguide facets.

Waveguide loss will occur due to the roughness of the waveguide and any material absorption through the SU-8. This attenuation was measured to be 21.15 dB/cm at 472 nm for waveguides with our dimensions using image processing software (ImageJ). A digital photograph was taken of fabricated test waveguides coupled to our blue laser source. The light intensity down the length of the waveguide was analyzed in order to determine the attenuation coefficient. Absorption through SU-8 at visible wavelengths is reported to be anywhere between 5 and 10 dB/cm at 472 nm [24,25], thus it is assumed that the rest of the waveguide loss is due to the roughness of the waveguide edges.

Divergence of the light is another possible source of loss as it crosses the microfluidic channel from one waveguide to the next. In such large core waveguides, it is very difficult to determine what modes the energy exists in at any given time. The following equations used to calculate the loss due to divergence assume the fundamental mode which can be approximated by a Gaussian beam. The spreading of a Gaussian beam as it leaves the facet of the waveguide can be calculated using:

$$w(z) = w_0\sqrt{1+\left(\frac{z}{z_o}\right)^2} \tag{2}$$

with

$$z_o = \frac{\pi w_0^2}{\lambda} \tag{3}$$

where $w(z)$ is the spot size of the beam after traveling a distance z in free space, w_0 is the beam waist as it leaves the waveguide and λ is the wavelength of light. The spreading of the beam width can be used to calculate the coupling efficiency of the light by using (4):

$$\eta = \frac{\left|\int_{-\infty}^{\infty} E_1(x,y) * E_2^*(x,y)\mathrm{d}x\ \mathrm{d}y\right|^2}{\int_{-\infty}^{\infty} E_1(x,y) * E_1^*(x,y)\mathrm{d}x\ \mathrm{d}y \int_{-\infty}^{\infty} E_2(x,y) * E_2^*(x,y)\mathrm{d}x\ \mathrm{d}y} \tag{4}$$

where $E(x,y)$ is the electromagnetic field strength in the x and y directions as the beam propagates in the z direction. By expressing the Gaussian beam formula in $E(x,y)$, the efficiency is found to be related to the spot size of the beam before and after traversing the channel:

$$\eta = \frac{2w(z)\times w_0}{w(z)^2 + w_0^2} \tag{5}$$

where $w(z)$ and w_0 are defined the same from (2) and (3). For the dimensions used in our device, the coupling efficiency of the light as it traverses the channel from one waveguide to another is near unity ($\eta = 0.99$). The high coupling efficiency is a result of using waveguides with large cross-sectional areas.

With these considerations, the most significant factor that contributes to optical loss in the device is the roughness of the waveguide facets and sides. This roughness contributes to over half of the total optical loss through the device. The waveguides were designed to have large cross-sectional areas to minimize the impact of divergence as light traverses the channel and to allow for easier coupling to the multimode optical fibers. The surface roughness of the waveguides is an inherent limitation when using lithography that cannot be completely avoided. Due to the loss already encountered using a single channel, a reference channel is not used for the experiment as this would require beam splitting which further increases the loss.

3. Device fabrication

3.1. Wafer level processes

The MEMS sensor was fabricated using conventional MEMS patterning techniques. Four-inch silicon wafers (⟨1 0 0⟩ orientation) begin with a 1-μm thick thermal SiO_2 to act as a bottom cladding layer for the waveguides. Layers of chrome (20 nm) and gold (200 nm) are sputtered onto the oxide coated wafers and patterned using Shipley 1813 photoresist to create the electrodes inside the microfluidic channels.

The lithography process for the SU-8 layer went through many optimization iterations. The mismatch in the coefficient of thermal expansion between the SU-8 and silicon coupled with the large footprint size of the devices make the film prone to delaminating throughout the fabrication process. SU-8 does not adhere well to oxide surfaces, therefore, an adhesion promoter, AP300 (Silicon Resources, Chandler, AZ) was used. The AP300 was first spun on the wafer at 5000 RPM and then baked on a hotplate at 150 °C for 15 min to remove solvent residues which the chemical otherwise left on the wafer. SU-8 was applied to the wafer and spun first at 600 RPM for 10 s followed by 1150 RPM for 30 s to achieve a final thickness of 100 μm. The heating procedure is not the conventional method for SU-8 and was developed in order to decrease the film stress as the wafer heats and cools. The pre-bake was performed on a hotplate at 55 °C for 2 h with a temperature ramp of 5°/min.

The SU-8 was exposed to UV light at a dose of 2500 mJ/cm^2 using a mask aligner system, and then placed back on the hotplate to bake at 55 °C for 90 min with a temperature ramp of 5°/min. After post-baking, the SU-8 was developed for 10 min in developer. The wafer was then immersed in a BOE 50:1 solution for 5 min to remove any TiO_2 particles left behind by the AP300 adhesion promoter as they were found to interfere with electrical contact. The next step involved patterning the sidewall waveguide facet with a transparent, conductive material to facilitate the chitosan deposition. Indium tin oxide (ITO) was deposited on the wafer using RF magnetron sputtering. The sidewall patterning procedure of the

Author's personal copy

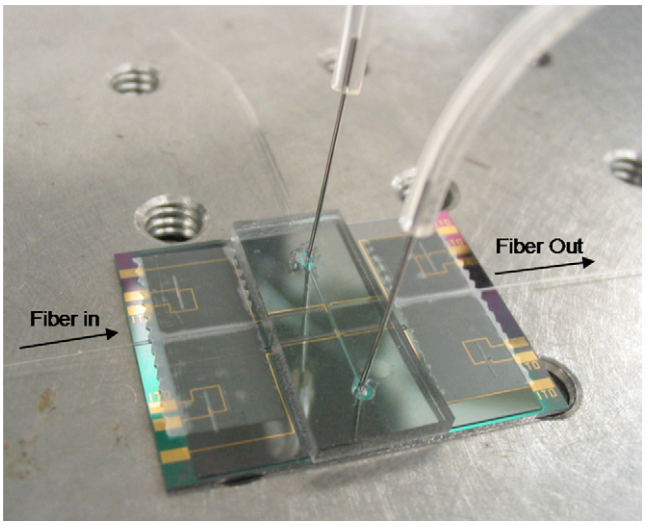

Fig. 4. Photo of fully packaged device including fluidic and optical connections. Two sensors are patterned in the same channel with only one currently being tested.

ITO using AZ9245 photoresist has been described elsewhere [26] and the results are shown in Fig. 3. The wafers are cleaned using acetone, methanol, isopropyl alcohol and DI water, then diced into individual dies for testing.

3.2. Die level processes

3.2.1. Chitosan deposition

Medium molecular weight (~200 kDa) chitosan flakes were purchased from Sigma–Aldrich and prepared using established methods resulting in a solution with pH of 5.3 and w/v chitosan of 0.5% [14]. The chitosan solution was applied to the active electrode area in the channel using a 100 μL syringe. It has been shown elsewhere that applying a current density of 4 A/m^2 results in a thin film deposition [27]. The surface area of the sidewall is not known and difficult to calculate. The deposition conditions were found empirically by applying varying current densities and observing the extent of chitosan sidewall coverage via SEM imaging. The currents were applied for 10 min, after which the device was rinsed extensively with DI water and blown dry with nitrogen. Applying a current of 0.35 μA results in complete chitosan coverage of the sidewall interface as seen in Fig. 2c. Applying currents higher than 1 μA causes bubble formation due to the evolution of excessive hydrogen gas at the cathode which disturbs the chitosan film formation.

After deposition, the moist chitosan films were measured to be between 5 and 10 μm by measuring the distance the chitosan extends from the sidewall using an optical microscope. Following a thorough rinse with DI water, the chips are immersed in a 1 M solution of NaOH for 5 min to neutralize the chitosan film.

3.2.2. Packaging

The fluidic channel was sealed using a thick (1 mm) flexible polymer, PDMS. PDMS is widely used for many microfluidic applications [28–30]. PDMS can be permanently bonded to oxide surfaces using a surface plasma treatment, but can also be reversibly bonded to other materials. PDMS curing agent and polymer were purchased from Sigma–Aldrich and mixed in a 1:10 ratio. The solution was cured at 80 °C for 25 min in a box furnace, and then cut into smaller pieces to fit over the device. To position the PDMS layer, methanol is applied to one side and the PDMS is slid into place over the device. The methanol evaporates and the PDMS is bonded to the SU-8. This bond was sufficient to hold the liquid pressures achieved during normal operation of the device and no leakage was detected.

The final packaged device is shown in Fig. 4. Metal capillaries with OD 400 μm and ID 200 μm were inserted through the PDMS to create liquid inlet and outlet ports. The capillaries fit snuggly within Tygon flexible tubing which was used to deliver the liquid to and from the device. Multimode optical fibers were aligned to the on-chip waveguides through the use of patterned grooves in the SU-8 resist. Once aligned by hand under a stereomicroscope, an adhesive was used to secure the fiber.

4. Testing and results

4.1. Macro-scale experiments

Testing the absorbance changes in the chitosan film due to catechol oxidation was performed using two methods. The first was to detect absorbance changes using a conventional UV–VIS spectrophotometer on chitosan films that had been dried onto glass slides. The second was to use the fabricated MEMS biosensor with an electrodeposited film of chitosan to detect the absorbance and compare the results.

Chitosan was cast onto glass slides with thickness of about 10 μm. The chitosan used for these experiments was 1.6% w/v in order to cast a thicker film. Following the casting, each slide was placed in 1 M NaOH for 5 min to neutralize the film and then washed extensively with DI water. Catechol flakes were purchased from Sigma–Aldrich and dissolved in a 20 mM phosphate buffer at a pH of 5.3 to create the catechol solutions. The slide experiments were performed by placing the chitosan-coated slide in contact with a gold electrode. A second gold electrode (cathode) along with the slide/electrode pair (anode) were placed in a beaker containing a predetermined concentration of catechol in buffer solution.

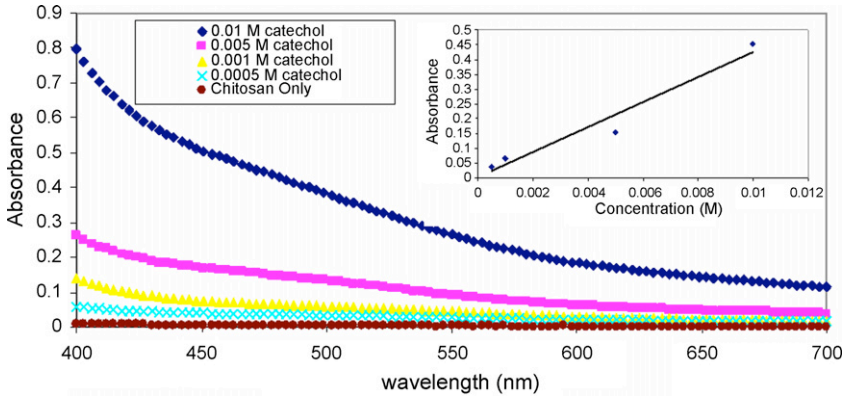

Fig. 5. Absorbance spectra for varying oxidized catechol concentrations. A clear increase in absorbance at low wavelengths for increasing concentration is observed. Inset graph displays the correlation between absorbance and concentration at the operating wavelength of 472 nm.

Author's personal copy

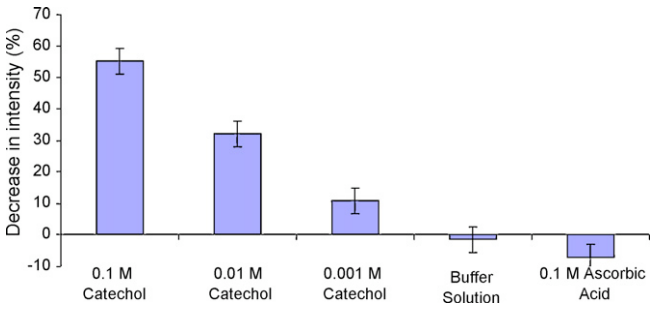

Fig. 6. Percent decrease in optical intensity after oxidizing various catechol concentrations and control fluids for 10 min each.

A 4 A/m^2 current density was applied to the anode for 10 min to allow for sufficient attachment of the generated *o*-quinones to the chitosan film.

The absorbance through the altered chitosan films with reference to a blank slide was measured using a GENESYS2 Spectrophotometer (Thermo Scientific, Waltham, MA). A relationship between the measured absorbance and the starting catechol concentration was observed as shown in Fig. 5. The inset graph shows that the absorbance is almost linear with concentration at 472 nm, the wavelength of light chosen to use for the MEMS device.

4.2. MEMS sensor experiments

Absorbance measurements from catechol oxidation were taken using blue light (472 nm) coupled through the MEMS device. Light was delivered from a free space blue laser (LaserMate, Pomona, CA) operating in the continuous wave mode and focused into a multimode fiber using a manual alignment stage. Output light was coupled via the optical fiber to a USB linked spectrophotometer (Ocean Optics, Dunedin, FL) which facilitated automated data collection using software. Catechol in buffer solution was prepared for each test using the same method as previously described. Liquid was administered using a GENIE PLUS syringe pump (Kent Scientific, Torrington, CT) at a flow rate of 100 μL/h, which translates to a linear flow velocity in the channel of about 1 mm/s.

Fig. 6 displays the decrease in measured light intensity for three different catechol concentrations after being oxidized for 10 min at a current density of 4 A/m^2. No increase in optical absorbance (decrease in light intensity) was observed from the oxidation of the buffer solution or the common reducing agent, ascorbic acid. Measurement error was calculated based on the observed fluctuations in the intensity measurement due to either change in the laser power or noise effects in the detector.

The increasing absorbance change over the 10 min period for each sample is displayed in Fig. 7. The accumulation of the *o*-quinones over time is diffusion limited as the catechol must traverse through the chitosan film to reach the electrode. Once again, it can be seen that ascorbic acid displays no absorbance increase throughout the duration of the reaction.

The use of the chitosan film is crucial in this application for amplifying the measured absorbance signal due to trapping of the *o*-quinones and for measuring low catechol concentrations. Fig. 8 displays the absorbance change over time without the chitosan film at the electrode interface in the channel when the same oxidizing current is applied. For higher catechol concentrations, the absorbance levels off after only two minutes, but is 69% and 82% less than the absorbance measurements taken when using the chitosan film in the channel for 0.1 and 0.01 M catechol respectively. No absorbance change is detected for the lower concentration of 0.001 M catechol. The absorbance level saturates as equilibrium is reached in the liquid between the creation of the *o*-quinones at the

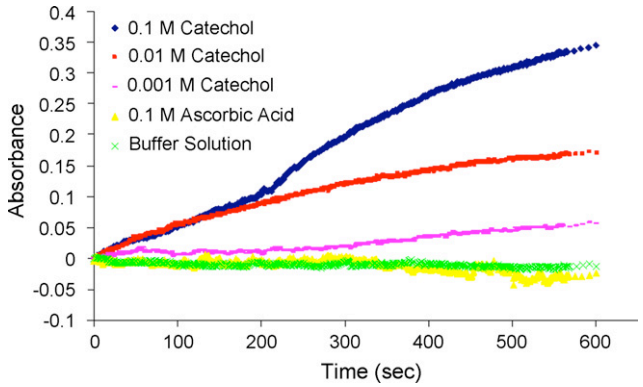

Fig. 7. Change in absorbance over 10 min reaction time for each sample.

electrode surface with the diffusion of the *o*-quinones away from the sensing area. It should be noted that the tests without chitosan require the liquid flow to be stopped in the channel. Any applied flow rate will cause the *o*-quinones to be swept away from the sensing area, disallowing any accumulation which would cause a detectable change in absorbance.

5. Discussion

The measured absorbance clearly increases with increasing catechol concentration for both the experiments performed using glass slides and those using the biosensor. Discrepancies between the data trends, including a non-linear absorbance relationship with concentration in the MEMS device, can most likely be attributed to variations in the sizes of the electrodes in the channel from device to device. The surface area variation can also be affected by the roughness of the ITO-coated polymer sidewall. These variations can not only cause irregular thicknesses of chitosan during the deposition, but can also slightly change the applied current density used to oxidize the catechol molecules. Further optimization of the fabrication procedure can help reduce this variability. Another possible source of error is the diffusion rate of the catechol through the chitosan matrix as more and more of the polymer is crosslinked by the *o*-quinones. The degree of crosslinking over a given time may not be linear if the diffusion rate of the catechol through the crosslinked region changes. The deviation from a linear relationship between concentration and absorbance can also be explained by strong molecular interactions at high concentrations [31]. Still, our biosensor data demonstrates general agreement with similar absorbance experiments performed in literature utilizing chitosan films where higher catechol concentrations (>10 mM) were also shown to have non-linear absorbance effects [32]. Since our device

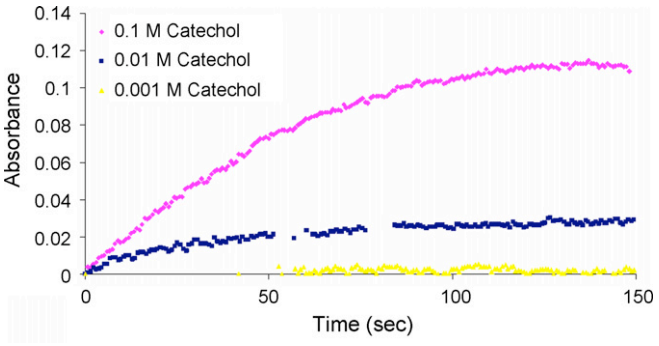

Fig. 8. Measured absorbance over reaction time without the chitosan film in the channel. The absorbance level saturates after 2 min and lower concentrations (<10 mM) are undetectable.

Author's personal copy

uniquely allows for the collection of time resolved absorbance data, calibration curves can be fit to different times in order to achieve more accurate sensing of the concentration. The absorbance change at lower catechol concentrations can be enhanced by increasing the reaction time.

The lack of any measurable signal in the presence of only a high concentration of ascorbic acid demonstrates the usefulness of an optical detection device for catechol. Although the ascorbic acid does become oxidized, its reduced form confers no absorbance change in the visible spectrum. The detection capabilities of the device may be affected by catechol in the presence of chemicals with low oxidation potentials and would vary based on the concentrations of each compound. Antioxidants in high enough concentrations relative to the catechol can also chemically reduce the *o*-quinones back into catechol molecules before they can bind to the amine groups of the chitosan film. One possible solution for achieving better selectivity in a solution with various samples is to apply different voltages to preferentially oxidize only those compounds with the desired oxidation potential as demonstrated in [33]. This procedure could allow for more selective catechol detection from real world samples such as tap water or lake water and is an area of future research with our biosensor.

This device represents the first step for using optical measurements in an on-chip sensor for catechol detection. The choice of materials for the device allow for the future integration of on-chip photodetectors. These photodetectors along with a small laser diode could be used with the current sensor design to create a truly portable system. Furthermore, many channels and waveguides can be patterned on a single chip for high-throughput screening of numerous samples.

6. Conclusion

We report the demonstration of on-chip catechol detection using optical absorbance measurements. We began with qualitatively identifying the absorbance change through chitosan films cast onto glass slides following exposure to varying concentrations of electrochemically oxidized catechol. The data exhibited a nearly linear relationship and provided a basis for comparison with the MEMS sensor results. The data collected from the MEMS sensor displays a slightly different correlation between the absorbance and the catechol concentration level than that from the experiments on the glass slides. This discrepancy is most likely due to fabrication variations between chips and can be improved. The device successfully demonstrates selective detection of phenolic (catechol) vs. non-phenolic (ascorbic acid) reducing compounds without using enzymes. This research provides the groundwork for detection of catechol and other phenolic compounds using a MEMS device packaged in a low-cost, portable system.

Acknowledgements

The authors gratefully acknowledge financial support from the R.W. Deutsch Foundation and the National Science Foundation (CBET-0650650 and EFRI-0735987).

References

[1] J. Shao, H. Ge, Y. Yang, Immobilization of polyphenol oxidase on chitosan-SiO_2 gel for removal of aqueous phenol, Biotechnology Letters 29 (2007) 901–905.
[2] C.T. Jung, R.R. Wickett, P.B. Desai, R.L. Bronaugh, In vitro and in vivo percutaneous absorption of catechol, Food and Chemical Toxicology 41 (2003) 885–895.
[3] A. Starek, Estrogens and organochlorine xenoestrogens and breast cancer risk, International Journal of Occupational Medicine and Environmental Health 16 (2003) 113–124.
[4] D.-P. Yang, H.-F. Ji, G.-Y. Tang, W. Ren, H.-Y. Zhang, How many drugs are catecholics, Molecules 12 (2007) 878–884.
[5] J. Abdullah, M. Ahmad, N. Karuppiah, L.Y. Heng, H. Sidek, Immobilization of tyrosinase in chitosan film for an optical detection of phenol, Sensors and Actuators B: Chemical 114 (2006) 604–609.
[6] X.J. Wu, M.M.F. Choi, X.M. Wu, An organic-phase optical phenol biosensor coupling enzymatic oxidation with chemical reduction, The Analyst 129 (2004) 1143–1149.
[7] M.J. Schöning, M. Jacobs, A. Muck, D.-T. Knobbe, J. Wang, M. Chatrathi, S. Spillmann, Amperometric PDMS/glass capillary electrophoresis-based biosensor microchip for catechol and dopamine detection, Sensors and Actuators B: Chemical vol.108 (2005) 688–694.
[8] D. Shan, M. Zhu, E. Han, H. Xue, S. Cosnier, Calcium carbonate nanoparticles: a host matrix for the construction of highly sensitive amperometric phenol biosensor, Biosensors and Bioelectronics 23 (2007) 648–654.
[9] S.M. Strawbridge, S.J. Green, J.H.R. Tucker, Electrochemical detection of catechol and dopamine as their phenylboronate ester derivatives, Chemistry Communication (2000) 2393–2394.
[10] J.K. Mbouguen, E. Ngameni, A. Walcarius, Quaternary ammonium functionalized clay film electrodes modified with polyphenol oxidase for the sensitive detection of catechol, Biosensors and Bioelectronics 23 (2007) 269–275.
[11] M.E. Kaoutit, I. Naranjo-Rodriguez, K.R. Temsamani, J.L.H.-H.D. Cisneros, The Sonogel-carbon materials as basis for development of enzyme biosensors for phenols and polyphenols monitoring: a detailed comparative study of three immobilization matrixes, Biosensors and Bioelectronics, 22, 2007, 2958–2966.
[12] L. Campanella, M.P. Sammartino, M. Tomassetti, New enzyme sensor for phenol determination in non-aqueous and aqueous medium, Sensors and Actuators B: Chemical 7 (1992) 383–388.
[13] G.F. Payne, M.V. Chaubal, T.A. Barbari, Enzyme-catalysed polymer modification: reaction of phenolic compounds with chitosan films, Polymer 37 (1996) 4643–4648.
[14] H. Yi, L.-Q. Wu, W.E. Bentley, R. Ghodssi, G.W. Rubloff, J.N. Culver, G.F. Payne, Biofabrication with chitosan, Biomacromolecules 6 (2005) 2881–2894.
[15] M. Luther, J. Parry, J. Moore, J. Meng, Y. Zhang, Z. Cheng, L. Yu, Inhibitory effect of Chardonnay and black raspberry seed extracts on lipid oxidation in fish oil and their radical scavenging and antimicrobial properties, Food Chemistry 104 (2007) 1065–1073.
[16] L. Su, J.-J. Yin, D. Charles, K. Zhou, J. Moore, L. Yu, Total phenolic contents, chelating capacities, and radical-scavenging properties of black peppercorn, nutmeg, rosehip, cinnamon and oregano leaf, Food Chemistry 100 (2005) 990–997.
[17] K. Zhou, J.-J. Yin, L. Yu, ESR determination of the reactions between selected phenolic acids and free radicals or transition metals, Food Chemistry 95 (2006) 446–457.
[18] H. Sies, Oxidative stress: oxidants and antioxidants, Experimental Physiology 82 (1997) 291–295.
[19] R.A. Zangmeister, J.J. Park, G.W. Rubloff, M.J. Tarlov, Electrochemical study of chitosan films deposited from solution at reducing potentials, Electrochimica Acta 51 (2006) 5324–5333.
[20] I. Park, J. Cheng, A.P. Pisano, E.-S. Lee, J.-H. Jeong, Low temperature, low pressure nanoimprinting of chitosan as a biomaterial for bionanotechnology applications, Applied Physics Letters 90 (2007).
[21] J.C. Cheng, A.P. Pisano, Photolithographic process for integration of the biopolymer chitosan into micro/nanostructures, Journal of Microelectricalmechanical Systems 17 (2008) 402–409.
[22] L.-Q. Wu, R. Ghodssi, Y.A. Elabd, G.F. Payne, Biomimetic pattern transfer, Advanced Functional Materials 15 (2005) 189–195.
[23] L.-Q. Wu, M.K. McDermott, C. Zhu, R. Ghodssi, G.F. Payne, Mimicking biological phenol reaction cascades to confer mechanical function, Advanced Functional Materials 16 (2006) 1967–1974.
[24] Z.-G. Ling, K. Lian, L. Jian, Improved patterning quality of SU-8 microstructures by optimizing the exposure parameters, in: Presented at SPIE: Advances in Resist Technology and Processing XVII, Santa Clara, CA, 2000.
[25] Microchem.
[26] M.A. Powers, S.T. Koev, A. Schleunitz, H. Yi, V. Hodzic, W.E. Bentley, G.F. Payne, G.W. Rubloff, R. Ghodssi, A fabrication platform for electrically mediated optically active biofunctionalized sites in BioMEMS, Lab Chip 5 (2005) 583–586.
[27] R. Fernandez, L.-Q. Wu, T. Chen, H. Yi, G.W. Rubloff, R. Ghodssi, W.E. Bentley, G.F. Payne, Electrochemically induced deposition of a polysaccharide hydrogel onto a patterned surface, Langmuir 19 (2003) 4058–4062.
[28] N. Nashida, W. Satoh, J. Fukuda, H. Suzuki, Electrochemical immunoassay on a microfluidic device with sequential injection and flushing functions, Biosensors and Bioelectronics 22 (2007) 3167–3173.
[29] J.M.K. Ng, I. Gitlin, A.D. Stroock, G.M. Whitesides, Components for integrated poly(dimethylsiloxane) microfluidic systems, Electrophoresis 23 (2002) 3461–3473.
[30] S.K. Sia, G.M. Whitesides, Microfluidic devices fabricated in poly(dimethylsiloxane) for biological studies, Electrophoresis 24 (2003) 3563–3576.
[31] J.R. Lakowicz, Principles of Fluorescence Spectroscopy, Plenum Press, New York, 1983.
[32] J. Abdullah, M. Ahmad, L.Y. Heng, N. Karuppiah, H. Sidek, An optical biosensor based on immobilization of laccase and MBTH in stacked films for the detection of catechol, Sensors 7 (2007) 2238–2250.
[33] Y. Liu, K.J. Gaskell, Z. Cheng, L. Yu, G.F. Payne, Chitosan-coated electrodes for bimodal sensing: selective post-electrode film reaction for spectroelectrochemical analysis, Langmuir 24 (2008) 7223–7231.

Author's personal copy

Biographies

Peter Dykstra received his BS degree in electrical engineering from Bucknell University in May, 2006. He received his MS degree in electrical engineering from the University of Maryland in October, 2008 and is currently there pursuing his PhD degree in electrical engineering. His research interests focus on microfluidic chemical and biological sensors utilizing immobilized polysaccharide films or DNA.

Junjie (George) Hao is currently a sophomore at the University of Maryland pursuing a double degree in Chemistry and Statistics. He is a Banneker/Key Scholar, and a part of the University of Maryland's Gemstone Program. His research interests are in analytical chemistry, particularly in subjects related to the promotion of human health.

Stephan Koev received a BS degree in electrical engineering from the US Naval Academy in 2004, and an MS degree in electrical engineering from the University of Maryland in 2007. He is currently a PhD candidate at the MEMS Sensors and Actuators Lab at the University of Maryland with a research focus on MEMS for biological applications. His interests include microfabrication, integrated optics, bio-device interfaces, and MEMS metrology.

Gregory F. Payne received his BS and MS degrees in Chemical Engineering from Cornell University in 1979 and 1981, respectively. He received his PhD in Chemical Engineering from The University of Michigan in 1984. After completing his PhD, he returned to Cornell to do post-doctoral work with Michael Shuler in biochemical engineering. In 1986 Dr. Payne joined the faculty with joint appointments in Chemical and Biochemical Engineering at the University of Maryland Baltimore County (UMBC) and in the Center for Agricultural Biotechnology (now the Center for Biosystems Research) at the University of Maryland Biotechnology Institute (UMBI). Currently he is a Professor and the Director of the Center for Biosystems Research. His research is focused on biofabrication – the use of biological or biomimetic materials and processes for construction. Specifically, his group biofabricates using enzymes and biologically derived polymers such as chitosan.

Liangli (Lucy) Yu received her MS in organic and medicinal chemistry in 1989 from China Pharmaceutical University and a PhD from Purdue University in 1999. She was an assistant professor in food science/food chemistry at Colorado State University from 1999–2003. In 2003, she joined the University of Maryland, College Park, as an assistant professor, and she has been an associate professor with the same university since 2005. She is interested in value-added nutraceuticals and functional foods, natural food preservatives, and nanodelivery and nanodetection systems for foods and nutraceuticals. She has edited two scientific books, coauthored 12 book chapters and more than 83 scientific articles, and is the primary inventor for 2 published patents. She serves on the editorial board for the *Molecular Nutrition and Food Research, Food Chemistry*, and the *LWT-Food Science and Technology*. She is the Membership Chair for Agricultural and Food Chemistry Division of the American Chemical Society. She has been the recipient of numerous awards including the 2006 Young Scientist Award from the American Chemical Society's Agricultural and Food Chemistry Division and the 2008 Young Scientist Research Award from the American Oil Chemist Society.

Reza Ghodssi is the Herbert Rabin Distinguished Associate Professor and Director of the MEMS Sensors and Actuators Lab (MSAL) in the Department of Electrical and Computer Engineering (ECE) and the Institute for Systems Research (ISR) at the University of Maryland (UMD). He is also affiliated with the Fischell Department of Bioengineering (BIOE), the Maryland NanoCenter, the University of Maryland Energy Research Center (UMERC), and the Materials Science and Engineering Department (MSE) at UMD. Dr. Ghodssi's research interests are in the design and development of microfabrication technologies and their applications to micro/nano devices and systems for chemical and biological sensing, small-scale energy conversion and harvesting. Dr. Ghodssi has over 62 scholarly publications, is the co-editor of the "Handbook of MEMS Materials and Processes" to be published in 2009, and is an associate editor for the Journal of Micorelectromechanical Systems (JMEMS) and Biomedical Microdevices (BMMD). Dr. Ghodssi has received the 2001 UMD George Corcoran Award, the 2002 National Science Foundation CAREER Award, and the 2003 UMD Outstanding Systems Engineering Faculty Award. Dr. Ghodssi is the co-founder of MEMS Alliance in the greater Washington area and a member of the IEEE, AVS, MRS, ASEE and AAAS societies.